mathematics

MDPI

Article

Variable Dose-Constraints Method Based on Multiplicative Dynamical Systems for High-Precision Intensity-Modulated Radiation Therapy Planning

Omar M. Abou Al-Ola [1], Takeshi Kojima [2], Ryosei Nakada [3], Norihisa Obata [4], Kohei Hayashi [5] and Tetsuya Yoshinaga [2,*]

[1] Faculty of Science, Tanta University, El-Giesh St., Tanta 31527, Egypt; omr.aboualaela@science.tanta.edu.eg
[2] Institute of Biomedical Sciences, Tokushima University, 3-18-15 Kuramoto, Tokushima 770-8509, Japan; kojima@tokushima-u.ac.jp
[3] Radiation & Proton Therapy Office, Shizuoka Cancer Center, 1007 Shimonagakubo, Nagaizumi 411-8777, Japan; r.nakada@scchr.jp
[4] Graduate School of Health Sciences, Tokushima University, 3-18-15 Kuramoto, Tokushima 770-8509, Japan; c202326002@tokushima-u.ac.jp
[5] Department of Radiology, Takamatsu Red Cross Hospital, 4-1-3 bancho, Kagawa 760-0017, Japan; k.hayashitaka672@gmail.com
* Correspondence: yosinaga@medsci.tokushima-u.ac.jp

Abstract: An optimization framework that effectively balances dose–volume constraints and treatment objectives is required in intensity-modulated radiation therapy (IMRT) planning. In our previous work, we proposed a dynamical systems-based approach in which dose constraints, along with beam coefficients, are treated as state variables and dynamically evolve within a continuous-time system. This method improved the accuracy of the solution by dynamically adjusting the dose constraints, but it had a significant drawback. Specifically, because it is as an iterative process derived from discretization of a linear differential equation system using the additive Euler method, a lower-bound clipping procedure is required to prevent the state variables for both beam coefficients and dose constraints from taking negative values. This issue could prevent constrained optimization from functioning properly and undermine the feasibility of the treatment plan. To address this problem, we propose two types of multiplicative continuous-time dynamical system that inherently preserve the nonnegativity of the state variables. We theoretically prove that the initial value problem for these systems converges to a solution that satisfies the constraints of consistent IMRT planning. Furthermore, to ensure computational practicality, we derive discretized iterative schemes from the continuous-time systems and confirm that their iterations maintain nonnegativity. This framework eliminates the need for artificial clipping procedures and leads to the multiplicative variable dose-constraints method, which dynamically adjusts dose constraints during the optimization process. Finally, numerical experiments are conducted to support and illustrate the theoretical results, showing how the proposed method achieves high-precision IMRT planning while ensuring physically meaningful solutions.

Keywords: dynamical system; differential equation; optimization; stability of equilibrium; intensity-modulated radiation therapy; variable dose-constraints method

MSC: 34A38; 34D20; 37N40; 92C50

check for updates

Academic Editors: Ahmadjan Muhammadhaji and Maimaiti Yimamu

Received: 22 April 2025
Revised: 26 May 2025
Accepted: 27 May 2025
Published: 2 June 2025

Citation: Abou Al-Ola, O.M.; Kojima, T.; Nakada, R.; Obata, N.; Hayashi, K.; Yoshinaga, T. Variable Dose-Constraints Method Based on Multiplicative Dynamical Systems for High-Precision Intensity-Modulated Radiation Therapy Planning. *Mathematics* **2025**, *13*, 1852. https://doi.org/10.3390/math13111852

Copyright: © 2025 by the authors. Licensee MDPI, Basel, Switzerland. This article is an open access article distributed under the terms and conditions of the Creative Commons Attribution (CC BY) license (https://creativecommons.org/licenses/by/4.0/).

1. Introduction

Intensity-modulated radiation therapy [1–4] (IMRT) is a widely used technique in cancer treatment that offers high precision in controlling the intensity and angle of radiation beams. This precision enables delivery of a sufficient dose to the planned target volume (PTV) while minimizing the dose to surrounding healthy tissues and organs at risk (OARs). The main challenge in IMRT planning is optimizing the balance between maximizing the dose to the PTV and minimizing the exposure to OARs. Mathematically, this involves solving an optimization problem where the objective function [5–10] is defined over beam intensity coefficients, subject to dose–volume constraints [11] and other feasibility conditions [12–14]. While this problem is critical for treatment success, including dose–volume constraints results in non-convex and non-differentiable functions, as they involve computing the volume fraction receiving dose above or below a threshold. This threshold-based evaluation introduces discontinuities in the objective function, making the optimization problem computationally demanding and difficult to solve efficiently [15–18].

Previous studies have employed feasibility-seeking projection methods [19–23], which avoid the challenges of non-convexity by iteratively projecting solutions onto feasible regions defined by the constraints. These methods allow for the incorporation of dose–volume constraints without encountering the associated difficulties. However, traditional IMRT optimization methods typically use fixed dose constraints that remain unchanged throughout the optimization process. This static setting may limit the quality of the final treatment plan.

In our prior work [24], we proposed a dynamical systems-based method that dynamically adjusts the dose constraints during optimization to improve the precision of treatment planning. This method treats dose constraints alongside beam coefficients as state variables evolving within a continuous-time dynamical system [25–28]. While this approach has been shown to enhance solution precision, it has a key drawback: the optimization is governed by an iterative process derived from discretization of a linear differential equation system using the additive Euler method, which may yield negative values for beam coefficients and dose constraints due to the additive nature of the update, thereby requiring a lower bound clipping procedure. Such negative values are physically meaningless and may undermine the feasibility of the treatment plan.

To address this issue, the current study introduces a novel approach based on two types of continuous-time dynamical system that inherently preserve the nonnegativity of the state variables. We provide a theoretical analysis demonstrating that the proposed systems converge to solutions that satisfy the constraints of a consistent IMRT plan. Additionally, to maintain computational efficiency, we derive discretized iterative methods from the continuous-time system. This method, referred to as the multiplicative variable dose-constraints method, ensures that the beam coefficients and dose constraints remain nonnegative throughout the optimization process, eliminating the need for additional clipping procedures.

Through numerical experiments, we illustrate the theoretical results and show that our approach guarantees physically meaningful solutions while achieving high-precision IMRT planning.

2. IMRT Treatment Planning

A radiation oncologist performs IMRT planning to determine the PTV to be irradiated and the OARs to be spared. In IMRT, let J represent the total number of beamlets that have split off from the radiation beam, and this is calculated as the number of delivered beams multiplied by the number of beamlets in each beam head. The dose calculation problem, in matrix notation, has the following form:

$$D = Kx. \tag{1}$$

Here, $D \in R_+^I$, with R_+ denoting the set of nonnegative real numbers, is the dose vector whose components represent the total dose deposited in each voxel of the patient's three-dimensional volume, $x \in R_+^J$ is the vector of intensities in beamlets, and $K \in R_+^{I \times J}$ consists of all elements $((K)^j)_i$ representing the dose deposited in the ith voxel due to the unit intensity of the jth beamlet; it is called the dose influence matrix. If there are volumes of the PTV and OAR with I_1 and I_2 voxels, respectively, then D includes $D_1 \in R_+^{I_1}$ and $D_2 \in R_+^{I_2}$ as subvectors, while K includes $K_1 \in R_+^{I_1 \times J}$ and $K_2 \in R_+^{I_2 \times J}$ as submatrices. Let b_1^{L} and b_2^{U} denote the prescribed lower and upper dose limits for PTV and OAR, respectively, where $b_1^{\mathrm{L}} > 0$ and $b_2^{\mathrm{U}} \geqslant 0$. Furthermore, to prevent excessive irradiation within the PTV, we introduce an upper bound b_1^{U} such that $b_1^{\mathrm{U}} > b_1^{\mathrm{L}}$.

In the case described above, we prepare a dose vector consisting of two subvectors of D_1 for the upper and lower dose bounds on the PTV and a subvector of D_2 for the upper dose bound on OAR,

$$D := \begin{pmatrix} D_1 \\ D_1 \\ D_2 \end{pmatrix} \in R_+^I \tag{2}$$

with $I = 2I_1 + I_2$ and a dose influence matrix with the same corresponding blocks of D,

$$K := \begin{pmatrix} K_1 \\ K_1 \\ K_2 \end{pmatrix} \in R_+^{I \times J}. \tag{3}$$

A similar formulation can be used for multiple PTVs and OARs, as well as for additional upper and lower dose constraints.

We consider consistent and acceptable systems in which IMRT planning problems based on dose constraints and dose–volume constraints are individually solvable.

Definition 1. *For a given IMRT planning system* $\{(K_1, b_1^{\mathrm{U}}), (K_1, b_1^{\mathrm{L}}), (K_2, b_2^{\mathrm{U}})\}$*, define sets as follows:*

$$\begin{aligned} \mathcal{E}_1^{\mathrm{U}} &:= \{e \in R_+^J : (K_1\, e)_{i_1} \leqslant b_1^{\mathrm{U}}, i_1 = 1, 2, \ldots, I_1\}, \\ \mathcal{E}_1^{\mathrm{L}} &:= \{e \in R_+^J : (K_1\, e)_{i_1} \geqslant b_1^{\mathrm{L}}, i_1 = 1, 2, \ldots, I_1\}, \ \textit{and} \\ \mathcal{E}_2^{\mathrm{U}} &:= \{e \in R_+^J : (K_2\, e)_{i_2} \leqslant b_2^{\mathrm{U}}, i_2 = 1, 2, \ldots, I_2\}. \end{aligned}$$

The system is consistent if the set

$$\mathcal{E} := \mathcal{E}_1^{\mathrm{U}} \cap \mathcal{E}_1^{\mathrm{L}} \cap \mathcal{E}_2^{\mathrm{U}} \tag{4}$$

is nonempty; otherwise it is inconsistent.

Definition 2. *For a given* $x \in R_+^J$ *and sets of dose–volume constraints* $(K_1, b_1^{\mathrm{U}}, \zeta_1^{\mathrm{U}})$*,* $(K_1, b_1^{\mathrm{L}}, \zeta_1^{\mathrm{L}})$*, and* $(K_2, b_2^{\mathrm{U}}, \zeta_2^{\mathrm{U}})$*, where* $\zeta_1^{\mathrm{U}} \leqslant 1$*,* $\zeta_1^{\mathrm{L}} \leqslant 1$*, and* $\zeta_2^{\mathrm{U}} \leqslant 1$ *represent the prescribed proportion rates, the corresponding dose distribution is considered partially acceptable if the number of elements in each of the index sets*

$$\begin{aligned} \mathcal{I}_1^{\mathrm{U}}(x) &= \left\{ i_1 \in \{1, 2, \ldots, I_1\} \ : \ (K_1\, x)_{i_1} \leqslant b_1^{\mathrm{U}} \right\}, \\ \mathcal{I}_1^{\mathrm{L}}(x) &= \left\{ i_1 \in \{1, 2, \ldots, I_1\} \ : \ (K_1\, x)_{i_1} \geqslant b_1^{\mathrm{L}} \right\}, \ \textit{and} \\ \mathcal{I}_2^{\mathrm{U}}(x) &= \left\{ i_2 \in \{1, 2, \ldots, I_2\} \ : \ (K_2\, x)_{i_2} \leqslant b_2^{\mathrm{U}} \right\} \end{aligned} \tag{5}$$

exceeds the prescribed proportions of I_1, I_1, and I_2. Equivalently, the following inequalities hold for some x:

$$\begin{aligned} \eta_1^{\mathrm{U}}(x) &:= \frac{|\mathcal{I}_1^{\mathrm{U}}(x)|}{I_1} \quad \geqslant \quad \zeta_1^{\mathrm{U}}, \\ \eta_1^{\mathrm{L}}(x) &:= \frac{|\mathcal{I}_1^{\mathrm{L}}(x)|}{I_1} \quad \geqslant \quad \zeta_1^{\mathrm{L}}, \ \textit{and} \\ \eta_2^{\mathrm{U}}(x) &:= \frac{|\mathcal{I}_2^{\mathrm{U}}(x)|}{I_2} \quad \geqslant \quad \zeta_2^{\mathrm{U}} \end{aligned} \tag{6}$$

where $|\cdot|$ denotes the cardinality of a set.

We say that an IMRT planning system is acceptable if there exists a common beam set for which the dose distributions in the PTVs and OARs are partially acceptable for all dose–volume constraints.

Definition 3. *For a given IMRT planning system $\{(K_1, b_1^{\mathrm{U}}, \zeta_1^{\mathrm{U}}), (K_1, b_1^{\mathrm{L}}, \zeta_1^{\mathrm{L}}), (K_2, b_2^{\mathrm{U}}, \zeta_2^{\mathrm{U}})\}$, define the following sets:*

$$\begin{aligned} \mathcal{A}_1^{\mathrm{U}} &:= \{a \in R_+^J : \eta_1^{\mathrm{U}}(a) \geqslant \zeta_1^{\mathrm{U}}\}, \\ \mathcal{A}_1^{\mathrm{L}} &:= \{a \in R_+^J : \eta_1^{\mathrm{L}}(a) \geqslant \zeta_1^{\mathrm{L}}\}, \ \textit{and} \\ \mathcal{A}_2^{\mathrm{U}} &:= \{a \in R_+^J : \eta_2^{\mathrm{U}}(a) \geqslant \zeta_2^{\mathrm{U}}\}. \end{aligned}$$

The system is considered acceptable if the set

$$\mathcal{A} := \mathcal{A}_1^{\mathrm{U}} \cap \mathcal{A}_1^{\mathrm{L}} \cap \mathcal{A}_2^{\mathrm{U}} \tag{7}$$

is nonempty; otherwise it is unacceptable or partially acceptable.

It is considered that $\mathcal{E}$ is a special case of the set $\mathcal{A}$ with $\zeta_1^{\mathrm{U}} = 1$, $\zeta_1^{\mathrm{L}} = 1$, and $\zeta_2^{\mathrm{U}} = 1$. We can also say that if the IMRT planning system is consistent, then it is acceptable.

In the rest of this section, we introduce some notations that will be used later. The superscript $\top$ denotes the transpose of a matrix or vector. The notation $(\theta)_i$ represents the ith element of the vector θ, while $(\Theta)_i$ and $(\Theta)^j$ refer to the ith row and jth column vectors of the matrix Θ, respectively. $\mathrm{Log}(\theta)$ and $\mathrm{Exp}(\theta)$ are vector-valued functions defined as $\mathrm{Log}(\theta) := (\log(\theta_1), \log(\theta_2), \ldots, \log(\theta_\ell))^\top$ and $\mathrm{Exp}(\theta) := (\exp(\theta_1), \exp(\theta_2), \ldots, \exp(\theta_\ell))^\top$, respectively, where $\theta = (\theta_1, \theta_2, \ldots, \theta_\ell)^\top$. Finally, $\mathrm{diag}(\theta)$ denotes a diagonal matrix whose diagonal entries are the elements of the vector θ.

3. Proposed Dynamical System and Theoretical Results

Given an IMRT planning system $\{(K_1, b_1^{\mathrm{U}}), (K_1, b_1^{\mathrm{L}}), (K_2, b_2^{\mathrm{U}})\}$, define a vector $y \in R_+^{\bar{I}}$ that will be considered part of the variable dose constraints to be estimated. For the subsequent discussion, assume that the prescribed dose conditions (K_1, b_1^{L}) and (K_2, b_2^{U}) are selected with $\bar{I} = I_1 + I_2$, although other combinations can be used, provided that at most one condition is chosen for each PTV or OAR volume.

The variable dose-constraints method for solving the IMRT planning problem in a consistent case is defined to find the desired solution for beam weights $e \in \mathcal{E}$ and the corresponding dose constraints $\bar{K}\, e$, where

$$\bar{K} := \begin{pmatrix} K_1 \\ K_2 \end{pmatrix} \in R_+^{\bar{I} \times J}, \tag{8}$$

from the solutions for the beam weights $x \in R_+^J$ and variable dose constraints

$$y = \begin{pmatrix} y_1 \\ y_2 \end{pmatrix} \in R_+^{\bar{I}},$$

where $y_1 \in R_+^{I_1}$ and $y_2 \in R_+^{I_2}$, in relation to an initial value problem of the dynamical system when the IMRT system satisfies the consistent condition in the sense of Definition 1. Therefore, the goal is to obtain the unknown variables x and y by minimizing an appropriate cost function, which is zero when $x = e$ and $y = \bar{K}e$ for some $e \in \mathcal{E}$. To solve this, we consider the following cost function for $x \in R_+^J$ and $y \in R_+^{\bar{I}}$ with $e \in \mathcal{E}$:

$$\begin{aligned} V(x,y) &= \sum_{j=1}^{J} (\lambda)_j^{-1} \mathrm{KL}((e)_j, (x)_j) + \alpha^{-1} \sum_{i=1}^{\bar{I}} \mathrm{KL}((\bar{K}e)_i, (y)_i) \\ &= \sum_{j=1}^{J} (\lambda)_j^{-1} \left((e)_j \log \frac{(e)_j}{(x)_j} + (x)_j - (e)_j \right) \\ &\quad + \alpha^{-1} \sum_{i=1}^{\bar{I}} \left((\bar{K}e)_i \log \frac{(\bar{K}e)_i}{(y)_i} + (y)_i - (\bar{K}e)_i \right) \end{aligned} \tag{9}$$

where KL denotes the generalized Kullback–Leibler divergence [29], $(\lambda)_j$ is defined as

$$(\lambda)_j = \left(\sum_{i_1=1}^{I_1} ((K_1)^j)_{i_1} + \sum_{i=1}^{\bar{I}} ((\bar{K})^j)_i \right)^{-1}$$

for $j = 1, 2, \ldots, J$, and $\alpha > 0$ is a weighting parameter. Note that the cost function, Equation (9), is nonnegative for any $x \in R_+^J$ and $y \in R_+^{\bar{I}}$, and it equals zero if and only if $x = e$ and $y = \bar{K}e$.

Finally, let us introduce functions P_1^{U}, P_1^{L}, and P_2^{U} that will be used in the system defined in the next subsection:

$$\begin{aligned} (P_1^{\mathrm{U}}(D_1, b_1))_{i_1} &= \begin{cases} (D_1)_{i_1}, & \text{if } (D_1)_{i_1} \leqslant (b_1)_{i_1}, \\ (b_1)_{i_1}, & \text{otherwise} \end{cases} \\ (P_1^{\mathrm{L}}(D_1, b_1))_{i_1} &= \begin{cases} (D_1)_{i_1}, & \text{if } (D_1)_{i_1} \geqslant (b_1)_{i_1}, \\ (b_1)_{i_1}, & \text{otherwise} \end{cases} \\ (P_2^{\mathrm{U}}(D_2, b_2))_{i_2} &= \begin{cases} (D_2)_{i_2}, & \text{if } (D_2)_{i_2} \leqslant (b_2)_{i_2}, \\ (b_2)_{i_2}, & \text{otherwise} \end{cases} \end{aligned}$$

where $i_1 = 1, 2, \ldots, I_1$ and $i_2 = 1, 2, \ldots, I_2$, with $b_1 \in R_+^{I_1}$ and $b_2 \in R_+^{I_2}$. As a simplification, we define the function

$$\bar{P}(c,d) := \begin{pmatrix} P_1^{\mathrm{L}}(c_1, d_1) \\ P_2^{\mathrm{U}}(c_2, d_2) \end{pmatrix} \tag{10}$$

where

$$c = \begin{pmatrix} c_1 \\ c_2 \end{pmatrix} \in R_+^{\bar{I}} \quad \text{and} \quad d = \begin{pmatrix} d_1 \\ d_2 \end{pmatrix} \in R_+^{\bar{I}},$$

where $c_1, d_1 \in R_+^{I_1}$ and $c_2, d_2 \in R_+^{I_2}$.

3.1. Consistent Planning

This section presents the definition of the dynamical systems for the variable dose-constraints method and discusses its theoretical outcomes when the IMRT planning system is consistent.

Consider the initial-value problem for a continuous-time dynamical system with state variables $(x(t), y(t)) \in R_{++}^{J+\bar{I}}$ such that $V(x(t), y(t))$ is expected to decrease over time $t \geqslant 0$ along their solutions, where R_{++} denotes the set of positive real numbers. The system is described by

$$\begin{aligned} \frac{dx(t)}{dt} &= X(t) f(x(t), y(t)) \\ \frac{dy(t)}{dt} &= Y(t) g(x(t), y(t)) \end{aligned} \tag{11}$$

where X and Y represent $\mathrm{diag}(x)$ and $\mathrm{diag}(y)$, respectively, the function g is given by

$$g(x, y) := \alpha\big(\mathrm{Log}(\bar{P}(y, \bar{K}\, x)) - \mathrm{Log}(y)\big), \tag{12}$$

and f is a vector-valued function defined below. The initial states are set as $x(0) =: x^0 \in R_{++}^J$, $y_1(0) =: y_1^0 \in \mathcal{Y}_1$, and $y_2(0) =: y_2^0 \in \mathcal{Y}_2$, where

$$\begin{aligned} \mathcal{Y}_1 &:= \Big\{ y_1 \in R_{++}^{I_1} \,:\, (y_1)_{i_1} \geqslant b_1^{\mathrm{L}},\ i_1 = 1, 2, \ldots, I_1 \Big\} \text{ and} \\ \mathcal{Y}_2 &:= \Big\{ y_2 \in R_{++}^{I_2} \,:\, (y_2)_{i_2} \leqslant b_2^{\mathrm{U}},\ i_2 = 1, 2, \ldots, I_2 \Big\}. \end{aligned}$$

Next, we will examine two dynamical systems described by Equations (11) and (12) and distinguished by their type of vector field. In particular, the two systems are given by specifying the function f in Equation (11) as

$$\begin{aligned} f(x, y) \;:=\; & \Lambda K_1^\top \big(\mathrm{Log}(P_1^{\mathrm{U}}(K_1\, x, u_1\, b_1^{\mathrm{U}})) - \mathrm{Log}(K_1\, x)\big) \\ & + \Lambda \bar{K}^\top \big(\mathrm{Log}(\bar{P}(\bar{K}\, x, y)) - \mathrm{Log}(\bar{K}\, x)\big) \end{aligned} \tag{13}$$

or

$$\begin{aligned} f(x, y) \;:=\; & \mathrm{Log}\Big(\Lambda K_1^\top \,\mathrm{Exp}\big(\mathrm{Log}(P_1^{\mathrm{U}}(K_1\, x, u_1\, b_1^{\mathrm{U}})) - \mathrm{Log}(K_1\, x)\big) \\ & + \Lambda \bar{K}^\top \,\mathrm{Exp}\big(\mathrm{Log}(\bar{P}(\bar{K}\, x, y)) - \mathrm{Log}(\bar{K}\, x)\big)\Big) \end{aligned} \tag{14}$$

where Λ represents $\mathrm{diag}(\lambda)$, and u_1 is the all-ones vector with I_1 elements.

Moreover, for carrying out practical calculations, we will perform a first-order numerical discretization of the above autonomous differential equations to derive iterative formulae which allow us to obtain approximate solutions. These formulae share a unified iterative algorithm or discrete-time system, with state variables for beam weights $z(n)$ and variable dose constraints $w(n)$ as functions of the iteration number n (with $n = 0, 1, 2, \ldots, N-1$, where N is the total number of iterations):

$$\begin{aligned} z(n+1) &= Z(n)\,\mathrm{Exp}(h f(z(n), w(n))) \\ w(n+1) &= W(n)\,\mathrm{Exp}(h g(z(n), w(n))) \end{aligned} \tag{15}$$

with $z(0) = x^0 \in R_{++}^J$ and $w(0) = y^0 = (y_1^0, y_2^0) \in \mathcal{Y}_1 \times \mathcal{Y}_2 \subset R_{++}^{\bar{I}}$, where Z and W indicate $\mathrm{diag}(z)$ and $\mathrm{diag}(w)$, respectively. The iterative formula in Equation (15) corresponds to a multiplicative Euler discretization with a step size of $h > 0$ for the continuous-time system described in Equation (11). The multiplicative method is particularly effective because it

ensures that the positivity of the iterative states $(z(n), w(n))$ is maintained at each iteration by selecting initial values $z(0) = x^0$ and $w(0) = y^0$.

Note that the difference systems consisting of Equations (15) and (12) in which the function f is defined as either Equation (13) or Equation (14) are, respectively, similar to the multiplicative algebraic reconstruction technique [30,31] (MART) and the maximum-likelihood expectation-maximization [32,33] (MLEM) algorithm for computed tomography. Namely, in the first equation of Equation (15) for $h = 1$, if we replace $P_1^{\cup}$ and $\bar{P}$ with the measured projections and assume that K and z correspond to the projection operator and the pixel density of the image to be reconstructed, respectively, the iterative formulae describe the MART and MLEM reconstruction algorithms.

In the following, we present theoretical results on the behavior of the solution $(x(t), y(t))$ for the continuous-time dynamical system described by Equations (11) and (12) with f defined as either Equation (13) or Equation (14). First, we demonstrate that all solutions remain within the positive subspace.

Proposition 1. *For a dynamical system obeying Equations (11) and (12) with f defined as either Equation (13) or Equation (14), if the initial value (x^0, y^0) belongs to $R_{++}^{J+\bar{I}}$, then the solution $(\varphi(t, x^0, y^0), \psi(t, x^0, y^0))$ remains within $R_{++}^{J+\bar{I}}$ for all $t > 0$.*

Proof. Since the system can be expressed as

$$\begin{aligned} d(x(t))_j/dt &= (x(t))_j (f(x(t), y(t)))_j \\ d(y(t))_i/dt &= (y(t))_i (g(x(t), y(t)))_i \end{aligned}$$

with functions $(f)_j$ and $(g)_i$ for $j = 1, 2, \ldots, J$ and $i = 1, 2, \ldots, \bar{I}$, it follows that for any j and i, the solution satisfies $(d(\varphi)_j/dt, d(\psi)_i/dt) \equiv (0, 0)$ on the subspace where $((x)_j, (y)_i) \equiv (0, 0)$. This implies that the subspace is invariant, and due to the uniqueness of solutions to the initial-value problem, trajectories cannot pass through any invariant subspace. Consequently, any solution $(\varphi(t, x^0, y^0), \psi(t, x^0, y^0))$ of a system described by Equations (11) and (12) with f defined as either Equation (13) or Equation (14) remains in $R_{++}^{J+\bar{I}}$ for all $t > 0$, given the initial condition $(x^0, y^0) \in R_{++}^{J+\bar{I}}$. □

Next, we introduce a theorem establishing the stability of the equilibrium in the dynamical system. Before proceeding, we present a lemma required for the proof.

Lemma 1. *We define the index sets as follows:*

$$\breve{\mathcal{I}}_1^{\cup}(x) := \left\{ i_1 \in \{1, 2, \ldots, I_1\} \ : \ (P_1^{\cup}(K_1\, x, u_1\, b_1^{\cup}))_{i_1} = b_1^{\cup} \right\}, \tag{16}$$

$$\widehat{\mathcal{M}}(x, y) := \left\{ i \in \{1, 2, \ldots, \bar{I}\} \ : \ (\bar{P}(\bar{K}\, x, y))_i = (y)_i \right\}, \text{ and} \tag{17}$$

$$\widetilde{\mathcal{M}}(x, y) := \left\{ i \in \{1, 2, \ldots, \bar{I}\} \ : \ (\bar{P}(y, \bar{K}\, x))_i = (\bar{K}\, x)_i \right\}. \tag{18}$$

When none of these sets is empty, for some x and y distinct from $e \in \mathcal{E}$ and $\bar{K}\, e$, respectively, the following three properties hold.

(i) *For any $i_1 \in \breve{\mathcal{I}}_1^{\cup}(x)$, the condition $(K_1\, x)_{i_1} > b_1^{\cup} \geqslant (K_1\, e)_{i_1}$ is satisfied.*

(ii) *For any $i \in \widehat{\mathcal{M}}(x, y)$, when $i \leqslant I_1$, the condition $(K_1\, e)_i \geqslant (y_1)_i > (K_1\, x)_i$ holds, and when $i > I_1$, the condition $(K_2\, x)_{i_2} > (y_2)_{i_2} \geqslant (K_2\, e)_{i_2}$ holds, where $i_2 = i - I_1$.*

(iii) *For any $i \in \widetilde{\mathcal{M}}(x, y)$, when $i \leqslant I_1$, the conditions $(K_1\, e)_i \geqslant (y_1)_i$ and $(K_1\, x)_i \geqslant (y_1)_i$ hold. When $i > I_1$, the conditions $(y_2)_{i_2} \geqslant (K_2\, x)_{i_2}$ and $(y_2)_{i_2} \geqslant (K_2\, e)_{i_2}$ hold, where $i_2 = i - I_1$.*

On the other hand, when the index sets are empty, we have $x = e$ and $y = \bar{K}\, e$.

Proof. The condition in property (i) follows from the definitions of P_1^{U} and $\mathcal{E}_1^{\mathrm{U}}$. Moreover, the conditions in properties (ii) and (iii) come from the definition of $\bar{P}$ and the following characteristics of the variable $y(t)$. Specifically, the structure of the vector field $g(x, y)$, which determines the differential coefficients of y in Equation (11), ensures that $y(t)$ remains within the same subspace of $\mathcal{Y}_1 \times \mathcal{Y}_2$ as its initial value and that it has a limit point $\bar{K}\, e$ that is the boundary of the subspace. On the other hand, when the sets $\breve{\mathcal{I}}_1^{\mathrm{U}}(x)$ and $\widehat{\mathcal{M}}(x, y)$ are empty, it follows that $x \in \mathcal{E}$ or $x = e$. Furthermore, if the set $\breve{\mathcal{M}}(x, y)$ is also empty, then $y = \bar{K}\, e$. □

Assuming that the inverse problem of IMRT planning, which is to minimize the cost function V in Equation (9), is consistent, the equilibrium $(e, \bar{K}\, e) \in R_{++}^{J+\bar{I}}$ for the system of differential equations, Equations (11) and (12), with f defined as in Equation (13) or Equation (14) is asymptotically stable, as ensured by the Lyapunov theorem.

Theorem 1. *If the set $\mathcal{E}$ in Equation (4) is nonempty, the solutions (x, y) to the dynamical system defined by Equations (11) and (12) with f defined as in Equation (13), given positive initial values, asymptotically converge to $(e, \bar{K}\, e)$ for some $e \in \mathcal{E}$. The same holds for the dynamical system described by Equation (14).*

Proof. Any point $(e, \bar{K}\, e)$ where $e \in \mathcal{E}$ is an equilibrium of the system defined by Equations (11) and (12) with f defined as in Equation (13). Suppose that the function $V(x, y) \geqslant 0$ in Equation (9) is a Lyapunov candidate function. This function is well-defined because, according to Proposition 1, the state $(x(t), y(t))$ of this dynamical system stays within $R_{++}^{J+\bar{I}}$ for any t when positive initial values are chosen. The function can be rewritten as

$$V(x, y) = \sum_{j=1}^{J} (\lambda)_j^{-1} \int_{(e)_j}^{(x)_j} \frac{r - (e)_j}{r} dr + \alpha^{-1} \sum_{i=1}^{\bar{I}} \int_{(\bar{K}\, e)_i}^{(y)_i} \frac{s - (\bar{K}\, e)_i}{s} ds,$$

so the derivative $\dot{V}$ with respect to t along the solution trajectory of the system satisfies

$$\begin{aligned}
\dot{V}(x, y) &= -\sum_{j=1}^{J} ((x)_j - (e)_j)(K_1^{\top})_j (\mathrm{Log}(K_1\, x) - \mathrm{Log}(P_1^{\mathrm{U}}(K_1\, x, u_1\, b_1^{\mathrm{U}}))) \\
&\quad - \sum_{j=1}^{J} ((x)_j - (e)_j)(\bar{K}^{\top})_j (\mathrm{Log}(\bar{K}\, x) - \mathrm{Log}(\bar{P}(\bar{K}\, x, y))) \\
&\quad - \sum_{i=1}^{\bar{I}} ((y)_i - (\bar{K}\, e)_i)(\log((y)_i) - \log((\bar{P}(y, \bar{K}\, x))_i) \\
&= -(K_1\, x - K_1\, e)^{\top} (\mathrm{Log}(K_1\, x) - \mathrm{Log}(P_1^{\mathrm{U}}(K_1\, x, u_1\, b_1^{\mathrm{U}}))) \\
&\quad -(\bar{K}\, x - \bar{K}\, e)^{\top} (\mathrm{Log}(\bar{K}\, x) - \mathrm{Log}(\bar{P}(\bar{K}\, x, y))) \\
&\quad -(\bar{K}\, e - y)^{\top} (\mathrm{Log}(\bar{P}(y, \bar{K}\, x)) - \mathrm{Log}(y)) \\
&= -\sum_{i_1 \in \breve{\mathcal{I}}_1^{\mathrm{U}}(x)} ((K_1\, x)_{i_1} - (K_1\, e)_{i_1})(\log((K_1\, x)_{i_1}) - \log(b_1^{\mathrm{U}})) \\
&\quad - \sum_{i \in \widehat{\mathcal{M}}(x,y)} ((\bar{K}\, x)_i - (\bar{K}\, e)_i)(\log((\bar{K}\, x)_i) - \log((y)_i)) \\
&\quad - \sum_{i \in \breve{\mathcal{M}}(x,y)} ((\bar{K}\, e)_i - (y)_i)(\log((\bar{K}\, x)_i) - \log((y)_i)) \\
&\leqslant -\sum_{i_1 \in \breve{\mathcal{I}}_1^{\mathrm{U}}(x)} ((K_1\, x)_{i_1} - b_1^{\mathrm{U}})(\log((K_1\, x)_{i_1}) - \log(b_1^{\mathrm{U}}))
\end{aligned}$$

$$
\begin{aligned}
& - \sum_{i \in \widehat{\mathcal{M}}(x,y)} ((\bar{K}\,x)_i - (y)_i)(\log((\bar{K}\,x)_i) - \log((y)_i)) \\
& - \sum_{i \in \widetilde{\mathcal{M}}(x,y)} ((\bar{K}\,e)_i - (y)_i)(\log((\bar{K}\,x)_i) - \log((y)_i)) \\
= \; & - \sum_{i_1 \in \widetilde{\mathcal{I}}_1^{\mathrm{U}}(x)} (\mathrm{KL}((K_1\,x)_{i_1}, b_1^{\mathrm{U}}) + \mathrm{KL}(b_1^{\mathrm{U}}, (K_1\,x)_{i_1})) \\
& - \sum_{i \in \widehat{\mathcal{M}}(x,y)} (\mathrm{KL}((\bar{K}\,x)_i, (y)_i) + \mathrm{KL}((y)_i, (\bar{K}\,x)_i)) \\
& - \sum_{i \in \widetilde{\mathcal{M}}(x,y)} ((\bar{K}\,e)_i - (y)_i)(\log((\bar{K}\,x)_i) - \log((y)_i)) \\
\leqslant \; & 0,
\end{aligned}
$$

where the index sets defined in Lemma 1 serve as summation ranges, meaning that the sum is taken only over the index elements where the corresponding values are nonzero. The first inequality follows from Lemma 1 and the monotonicity of the logarithm function. In the final inequality, if $x = e$ and $y = \bar{K}\,e$, it is immediately evident that the derivative becomes 0. On the other hand, setting the left-hand side of this inequality to 0 requires all three index sets to be empty, which, according to Lemma 1, leads to $x = e$ and $y = \bar{K}\,e$. Therefore, the derivative equals 0 if and only if $x = e$ and $y = \bar{K}\,e$. This confirms that the solutions to the dynamical system described by Equations (11) and (12) with f defined as in Equation (13) asymptotically converge to some e in $\mathcal{E}$, as guaranteed by the Lyapunov theorem.

Similarly, it can be shown that V also serves as a Lyapunov function for the dynamical system described by Equations (11) and (12) with f defined as in Equation (14). The derivative $\dot{V}$ of V with respect to t along the system's dynamics is given by

$$
\begin{aligned}
\dot{V}(x,y) \; = \; & - \sum_{j=1}^{J} ((e)_j - (x)_j)(\lambda)_j^{-1} \log\Big((\lambda)_j (K_1^\top)_j \operatorname{Exp}(\operatorname{Log}(P_1^{\mathrm{U}}(K_1\,x, u_1\,b_1^{\mathrm{U}})) - \operatorname{Log}(K_1\,x)) \\
& \qquad + (\lambda)_j (\bar{K}^\top)_j \operatorname{Exp}(\operatorname{Log}(\bar{P}(\bar{K}\,x, y)) - \operatorname{Log}(\bar{K}\,x)) \Big) \\
& - \sum_{i=1}^{\bar{I}} ((y)_i - (\bar{K}\,e)_i)(\log((y)_i) - \log((\bar{P}(y, \bar{K}\,x))_i)) \\
\leqslant \; & - \sum_{j=1}^{J} (e)_j (K_1^\top)_j (\operatorname{Log}(P_1^{\mathrm{U}}(K_1\,x, u_1\,b_1^{\mathrm{U}})) - \operatorname{Log}(K_1\,x)) \\
& - \sum_{j=1}^{J} (e)_j (\bar{K}^\top)_j (\operatorname{Log}(\bar{P}(\bar{K}\,x, y)) - \operatorname{Log}(\bar{K}\,x)) \\
& + \sum_{j=1}^{J} (x)_j (\lambda)_j^{-1} \Big((\lambda)_j (K_1^\top)_j \operatorname{Exp}(\operatorname{Log}(P_1^{\mathrm{U}}(K_1\,x, u_1\,b_1^{\mathrm{U}})) - \operatorname{Log}(K_1\,x)) \\
& \qquad + (\lambda)_j (\bar{K}^\top)_j \operatorname{Exp}(\operatorname{Log}(\bar{P}(\bar{K}\,x, y)) - \operatorname{Log}(\bar{K}\,x)) - 1 \Big) \\
& - \sum_{i=1}^{\bar{I}} ((\bar{K}\,e)_i - (y)_i)(\log((\bar{P}(y, \bar{K}\,x))_i) - \log((y)_i)) \\
\leqslant \; & -(K_1\,e)^\top (u_1 - \operatorname{Exp}(\operatorname{Log}(K_1\,x) - \operatorname{Log}(P_1^{\mathrm{U}}(K_1\,x, u_1\,b_1^{\mathrm{U}})))) \\
& -(\bar{K}\,e)^\top \left(\bar{u} - \operatorname{Exp}(\operatorname{Log}(\bar{K}\,x) - \operatorname{Log}(\bar{P}(\bar{K}\,x, y)))\right) \\
& +(K_1\,x)^\top (\operatorname{Exp}(\operatorname{Log}(P_1^{\mathrm{U}}(K_1\,x, u_1\,b_1^{\mathrm{U}})) - \operatorname{Log}(K_1\,x)) - u_1) \\
& +(\bar{K}\,x)^\top \left(\operatorname{Exp}(\operatorname{Log}(\bar{P}(\bar{K}\,x, y)) - \operatorname{Log}(\bar{K}\,x)) - \bar{u}\right)
\end{aligned}
$$

$$
\begin{aligned}
& -(\bar{K}\,e - y)^{\top}(\mathrm{Log}(\bar{P}(y, \bar{K}\,x)) - \mathrm{Log}(y)) \\
= & -\sum_{i_1 \in \check{\mathcal{I}}_1^{\mathrm{U}}(x)} (K_1\,e)_{i_1}\left(1 - \exp(\log((K_1\,x)_{i_1}) - \log(b_1^{\mathrm{U}}))\right) \\
& +\sum_{i_1 \in \check{\mathcal{I}}_1^{\mathrm{U}}(x)} (K_1\,x)_{i_1}\left(\exp(\log(b_1^{\mathrm{U}}) - \log((K_1\,x)_{i_1})) - 1\right) \\
& -\sum_{i \in \widehat{\mathcal{M}}(x,y)} (\bar{K}\,e)_i(1 - \exp(\log((\bar{K}\,x)_i) - \log((y)_i))) \\
& +\sum_{i \in \widehat{\mathcal{M}}(x,y)} (\bar{K}\,x)_i\left(\exp(\log((y)_i) - \log((\bar{K}\,x)_i)) - 1\right) \\
& -\sum_{i \in \widetilde{\mathcal{M}}(x,y)} ((\bar{K}\,e)_i - (y)_i)(\log((\bar{K}\,x)_i) - \log((y)_i)) \\
= & -\sum_{i_1 \in \check{\mathcal{I}}_1^{\mathrm{U}}(x)} \frac{1}{b_1^{\mathrm{U}}}\left(b_1^{\mathrm{U}} - (K_1\,e)_{i_1}\right)\left((K_1\,x)_{i_1} - b_1^{\mathrm{U}}\right) \\
& -\sum_{i \in \widehat{\mathcal{M}}(x,y)} \frac{1}{(y)_i}\left((y)_i - (\bar{K}\,e)_i\right)\left((\bar{K}\,x)_i - (y)_i\right) \\
& -\sum_{i \in \widetilde{\mathcal{M}}(x,y)} ((\bar{K}\,e)_i - (y)_i)(\log((\bar{K}\,x)_i) - \log((y)_i)) \\
\leqslant & \ 0
\end{aligned}
$$

where u_1 and $\bar{u}$ represent all-ones vectors with I_1 and $\bar{I}$ elements, respectively. As in the previous case, the index sets used as the summation ranges are defined by Lemma 1. Here, the first inequality is obtained using the concavity of the logarithmic function and Jensen's inequality, along with the fact that $\log(\theta) \leqslant \theta - 1$ for any nonnegative θ. The second inequality follows from the relation $\theta \leqslant \exp(\theta) - 1$ for any θ. The derivatives become zero if and only if $x = e$ and $y = \bar{K}\,e$. Therefore, the solutions to the dynamical system obeying Equations (11) and (12) with f defined as in (14) asymptotically converge to some $e \in \mathcal{E}$. □

3.2. Acceptable Planning

For an acceptable IMRT planning system, the two iterative algorithms of the variable dose-constraints method by using a multiplicative iterative scheme can be written in the following unified form.

$$
\begin{aligned}
z(n+1) &= Z(n)\,\mathrm{Exp}(hp(z(n), w(n))) \\
w_1(n+1) &= W_1(n)\,\mathrm{Exp}(hq_1(z(n), w_1(n))) \\
w_2(n+1) &= W_2(n)\,\mathrm{Exp}(hq_2(z(n), w_2(n)))
\end{aligned} \tag{19}
$$

for $n = 0, 1, 2, \ldots, N-1$ with $z(0) = x^0 \in R^I_{++}$ and $w(0) = y^0 \in \mathcal{Y}_1 \times \mathcal{Y}_2$, where w_1 and w_2 are subvectors defined by

$$
w = \begin{pmatrix} w_1 \\ w_2 \end{pmatrix},
$$

W_1 and W_2 denote $\mathrm{diag}(w_1)$ and $\mathrm{diag}(w_2)$, respectively, and $h > 0$ denotes a step-size parameter. As preparation for defining the functions p and $q = (q_1, q_2)$, we introduce the following binary functions, referred to as acceptable indices, with respect to the beam coefficient variable $x \in R^J_+$ according to Definition 2.

$$
\delta_1^{\mathrm{U}}(x) = \begin{cases} 0, & \text{if } x \text{ with } (K_1,\, b_1^{\mathrm{U}},\, \zeta_1^{\mathrm{U}}) \text{ is partially acceptable,} \\ \mu_1^{\mathrm{U}}, & \text{otherwise} \end{cases} \tag{20}
$$

$$\delta_1^{\mathrm{L}}(x) = \begin{cases} 0, & \text{if } x \text{ with } (K_1, b_1^{\mathrm{L}}, \zeta_1^{\mathrm{L}}) \text{ is partially acceptable,} \\ \mu_1^{\mathrm{L}}, & \text{otherwise} \end{cases} \tag{21}$$

$$\delta_2^{\mathrm{U}}(x) = \begin{cases} 0, & \text{if } x \text{ with } (K_2, b_2^{\mathrm{U}}, \zeta_2^{\mathrm{U}}) \text{ is partially acceptable,} \\ \mu_2^{\mathrm{U}}, & \text{otherwise} \end{cases} \tag{22}$$

where the positive values μ_1^{U}, μ_1^{L}, and μ_2^{U} are penalty coefficients that weight the importance of each constraint, and their setting takes into account that they are multiplied by the step size h. Furthermore, to quantify the interaction between IMRT subsystems, we define the following metric, referred to as the collaboration index:

$$\Delta(x) := \delta_1^{\mathrm{U}}(x) + \delta_1^{\mathrm{L}}(x) + \delta_2^{\mathrm{U}}(x), \tag{23}$$

for a given x. The function p is defined according to two multiplicative types: the multiplicative algebraic (MA) type, where

$$\begin{aligned} p(z,w) := {} & \delta_1^{\mathrm{U}}(z)\Lambda K_1^{\top}(\mathrm{Log}(P_1^{\mathrm{U}}(K_1\, z, u_1\, b_1^{\mathrm{U}})) - \mathrm{Log}(K_1\, z)) \\ & + \delta_1^{\mathrm{L}}(z)\Lambda K_1^{\top}(\mathrm{Log}(P_1^{\mathrm{L}}(K_1\, z, w_1)) - \mathrm{Log}(K_1\, z)) \\ & + \delta_2^{\mathrm{U}}(z)\Lambda K_2^{\top}(\mathrm{Log}(P_2^{\mathrm{U}}(K_2\, z, w_2)) - \mathrm{Log}(K_2\, z)) \end{aligned} \tag{24}$$

and the expectation maximization (EM) type, where

$$\begin{aligned} p(z,w) := {} & \delta_1^{\mathrm{U}}(z)\,\mathrm{Log}\Big(\Lambda K_1^{\top}\,\mathrm{Exp}(\mathrm{Log}(P_1^{\mathrm{U}}(K_1\, z, u_1\, b_1^{\mathrm{U}})) - \mathrm{Log}(K_1\, z))\Big) \\ & + \delta_1^{\mathrm{L}}(z)\,\mathrm{Log}\Big(\Lambda K_1^{\top}\,\mathrm{Exp}(\mathrm{Log}(P_1^{\mathrm{L}}(K_1\, z, w_1)) - \mathrm{Log}(K_1\, z))\Big) \\ & + \delta_2^{\mathrm{U}}(z)\,\mathrm{Log}\Big(\Lambda K_2^{\top}\,\mathrm{Exp}(\mathrm{Log}(P_2^{\mathrm{U}}(K_2\, z, w_2)) - \mathrm{Log}(K_2\, z))\Big). \end{aligned} \tag{25}$$

Finally, the function q is defined as

$$q_1(z, w_1) := \alpha\delta_1^{\mathrm{L}}(z)(\mathrm{Log}(P_1^{\mathrm{L}}(w_1, K_1\, z)) - \mathrm{Log}(w_1)) \tag{26}$$

$$q_2(z, w_2) := \alpha\delta_2^{\mathrm{U}}(z)(\mathrm{Log}(P_2^{\mathrm{U}}(w_2, K_2\, z)) - \mathrm{Log}(w_2)). \tag{27}$$

The positivity of the iterative solution produced by Equation (19) is clear. Specifically, since the initial values are chosen to be positive, the elements of $z(n)$ and $w(n)$ will remain positive for any iteration n, regardless of the multiplicative type.

Consider a situation where the system $\{(K_1, b_1^{\mathrm{U}}, \zeta_1^{\mathrm{U}}), (K_1, b_1^{\mathrm{L}}, \zeta_1^{\mathrm{L}}), (K_2, b_2^{\mathrm{U}}, \zeta_2^{\mathrm{U}})\}$ is inconsistent and acceptable. In this case, Equation (19) describes a subsystem obtained by deactivating certain terms from the original complete system, Equation (15). For example, when the dose distribution of the dose–volume constraints $(K_1, b_1^{\mathrm{U}}, \zeta_1^{\mathrm{U}})$, $(K_1, b_1^{\mathrm{L}}, \zeta_1^{\mathrm{L}})$, and $(K_2, b_2^{\mathrm{U}}, \zeta_2^{\mathrm{U}})$ becomes partially acceptable, the corresponding acceptable indices $\delta_1^{\mathrm{U}}(x)$, $\delta_1^{\mathrm{L}}(x)$, and $\delta_2^{\mathrm{U}}(x)$ become 0. Consequently, the associated constraint terms are rendered inactive, leading to a reduced subsystem. Thus, Equation (19) can be interpreted as a switching system whose structure changes depending on the values of the state variables. That is, as the state variables evolve, certain constraints become inactive, altering the influence of the constraints and causing the overall system behavior to switch accordingly.

The process by which the entire system reaches an acceptable state can be explained as follows. In two target structures traversed by common beams, variations in the beam coefficients can have opposing effects on their respective dose constraints. We refer to this phenomenon as a "competitive effect". When a competitive effect occurs, as the dose of one target structure approaches its constraint, the dose of the other structure moves away from its own constraint. However, once a constraint is sufficiently satisfied and the system

reaches a partially acceptable state, the corresponding constraint term is deactivated, thereby altering the system dynamics. Specifically, the solution trajectory proceeds in accordance with a simplified subsystem composed of the remaining active constraints. By repeating this process, different constraints are alternately optimized, eventually leading the entire system to converge to an acceptable state. Throughout this process, despite the presence of competition, the influence of the constraints shifts in a manner that promotes optimization. This results in the emergence of a "cooperative effect", where constraints work together to guide the system toward an optimal solution.

4. Experiments

We show through experiments that the proposed variable dose-constraints method, based on the multiplicative MA-type and EM-type iterative formulae, operates as expected and performs better than the additive iterative formula presented in the previous study [24].

4.1. Method

The phantom encompassed a Core (blue region), a C-shaped Target (red region), and a Body (dark-gray region); here, the reader is referred to the C-shaped phantom detailed in the task group 119 (TG119) report by the American Association of Physicists in Medicine (AAPM). An image of the phantom is shown in Figure 1. The IMRT planning used in this study follows a slightly stricter formulation than the acceptable planning presented in Reference [24]. The dose–volume constraints prescribed for the planning system $\left\{(K_{\mathrm{C}}, b_{\mathrm{C}}^{\mathrm{U}}, \zeta_{\mathrm{C}}^{\mathrm{U}}), (K_{\mathrm{T}}, b_{\mathrm{T}}^{\mathrm{U}}, \zeta_{\mathrm{T}}^{\mathrm{U}}), (K_{\mathrm{T}}, b_{\mathrm{T}}^{\mathrm{L}}, \zeta_{\mathrm{T}}^{\mathrm{L}}), (K_{\mathrm{B}}, b_{\mathrm{B}}^{\mathrm{U}}, \zeta_{\mathrm{B}}^{\mathrm{U}})\right\}$ are summarized in Table 1, where V_d denotes the percentage of volume receiving at least the dose d (in Gy), and these constraints are used throughout the study unless otherwise stated. In these expressions, superscripts U and L denote upper and lower limits, respectively, while subscripts C, T, and B indicate the Core, Target, and Body regions, respectively. The treatment planning utilized nine beam angles, evenly spaced at 40-degree intervals, spanning 0 to 360 degrees (J = 2492). The voxel counts for the Core, Target, and Body were $I_{\mathrm{C}} = 1089$, $I_{\mathrm{T}} = 6275$, and $I_{\mathrm{B}} = 495{,}116$, respectively. Variable dose constraints w_{C} and w_{T} were defined as $w := (w_{\mathrm{C}}, w_{\mathrm{T}}) \in R_{++}^{I_{\mathrm{C}}+I_{\mathrm{T}}}$ to correspond to the prescribed dose conditions $(K_{\mathrm{C}}, b_{\mathrm{C}}^{\mathrm{U}})$ and $(K_{\mathrm{T}}, b_{\mathrm{T}}^{\mathrm{L}})$, respectively.

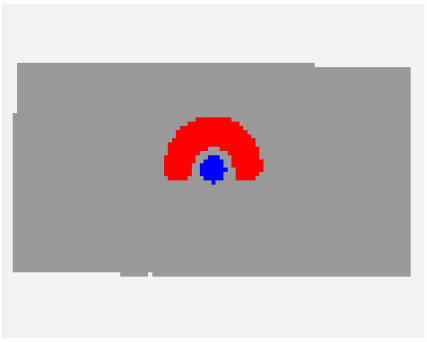


Figure 1. Phantom image of C-shape (red region represents Target as PTV, while blue and dark-gray regions, respectively, represent Core and Body as OARs).

Table 1. Prescribed constraints and equivalent parameters for acceptable IMRT treatment planning system.

Assigned Region (Colored Region in Figure 1)	Organ	Constraint [%]	Equivalent Parameter
OAR (blue)	Core	$V_{15} < 5$	$(K_{\mathrm{C}}, b_{\mathrm{C}}^{\mathrm{U}}, \zeta_{\mathrm{C}}^{\mathrm{U}})$ with $b_{\mathrm{C}}^{\mathrm{U}} = 15$ and $\zeta_{\mathrm{C}}^{\mathrm{U}} = 0.95$
PTV (red)	Target	$V_{55} < 10$	$(K_{\mathrm{T}}, b_{\mathrm{T}}^{\mathrm{U}}, \zeta_{\mathrm{T}}^{\mathrm{U}})$ with $b_{\mathrm{T}}^{\mathrm{U}} = 55$ and $\zeta_{\mathrm{T}}^{\mathrm{U}} = 0.90$
		$V_{50} \geqslant 95$	$(K_{\mathrm{T}}, b_{\mathrm{T}}^{\mathrm{L}}, \zeta_{\mathrm{T}}^{\mathrm{L}})$ with $b_{\mathrm{T}}^{\mathrm{L}} = 50$ and $\zeta_{\mathrm{T}}^{\mathrm{L}} = 0.95$
OAR (dark gray)	Body	$V_{20} < 20$	$(K_{\mathrm{B}}, b_{\mathrm{B}}^{\mathrm{U}}, \zeta_{\mathrm{B}}^{\mathrm{U}})$ with $b_{\mathrm{B}}^{\mathrm{U}} = 20$ and $\zeta_{\mathrm{B}}^{\mathrm{U}} = 0.80$

The iterative algorithm of the MA-type variable dose-constraints method is derived by transforming Equation (19) on the basis of the given dose constraint conditions. It can be expressed using the following simultaneous recurrence equations for the variables $z \in R^{I}_{++}$, $w_{\mathrm{C}} \in R^{I_{\mathrm{C}}}_{++}$, and $w_{\mathrm{T}} \in R^{I_{\mathrm{T}}}_{++}$:

$$\begin{aligned} z(n+1) &= Z(n)\,\mathrm{Exp}(p(z(n), w(n))) \\ w_{\mathrm{C}}(n+1) &= W_{\mathrm{C}}(n)\,\mathrm{Exp}(\alpha q_{\mathrm{C}}(z(n), w_{\mathrm{C}}(n))) \\ w_{\mathrm{T}}(n+1) &= W_{\mathrm{T}}(n)\,\mathrm{Exp}(\alpha q_{\mathrm{T}}(z(n), w_{\mathrm{T}}(n))) \end{aligned} \tag{28}$$

for $n = 0, 1, 2, \ldots, N-1$, where

$$p(z, w) := \delta^{\mathrm{U}}_{\mathrm{C}}(z) p^{\mathrm{U}}_{\mathrm{C}}(z, w_{\mathrm{C}}) + \delta^{\mathrm{U}}_{\mathrm{T}}(z) p^{\mathrm{U}}_{\mathrm{T}}(z) + \delta^{\mathrm{L}}_{\mathrm{T}}(z) p^{\mathrm{L}}_{\mathrm{T}}(z, w_{\mathrm{T}}) + \delta^{\mathrm{U}}_{\mathrm{B}}(z) p^{\mathrm{U}}_{\mathrm{B}}(z) \tag{29}$$

with

$$p^{\mathrm{U}}_{\mathrm{C}}(z, w_{\mathrm{C}}) := \Lambda K_{\mathrm{C}}^{\top}(\mathrm{Log}(P^{\mathrm{U}}_{\mathrm{C}}(K_{\mathrm{C}}\, z, w_{\mathrm{C}})) - \mathrm{Log}(K_{\mathrm{C}}\, z)) \tag{30}$$

$$p^{\mathrm{U}}_{\mathrm{T}}(z) := \Lambda K_{\mathrm{T}}^{\top}(\mathrm{Log}(P^{\mathrm{U}}_{\mathrm{T}}(K_{\mathrm{T}}\, z, u_{\mathrm{T}}\, b^{\mathrm{U}}_{\mathrm{T}})) - \mathrm{Log}(K_{\mathrm{T}}\, z)) \tag{31}$$

$$p^{\mathrm{L}}_{\mathrm{T}}(z, w_{\mathrm{T}}) := \Lambda K_{\mathrm{T}}^{\top}(\mathrm{Log}(P^{\mathrm{L}}_{\mathrm{T}}(K_{\mathrm{T}}\, z, w_{\mathrm{T}})) - \mathrm{Log}(K_{\mathrm{T}}\, z)) \tag{32}$$

$$p^{\mathrm{U}}_{\mathrm{B}}(z) := \Lambda K_{\mathrm{B}}^{\top}(\mathrm{Log}(P^{\mathrm{U}}_{\mathrm{B}}(K_{\mathrm{B}}\, z, u_{\mathrm{B}}\, b^{\mathrm{U}}_{\mathrm{B}})) - \mathrm{Log}(K_{\mathrm{B}}\, z)) \tag{33}$$

and

$$q_{\mathrm{C}}(z, w_{\mathrm{C}}) := \delta^{\mathrm{U}}_{\mathrm{C}}(z) q^{\mathrm{U}}_{\mathrm{C}}(z, w_{\mathrm{C}}) \tag{34}$$

$$q_{\mathrm{T}}(z, w_{\mathrm{T}}) := \delta^{\mathrm{L}}_{\mathrm{T}}(z) q^{\mathrm{L}}_{\mathrm{T}}(z, w_{\mathrm{T}}) \tag{35}$$

with

$$q^{\mathrm{U}}_{\mathrm{C}}(z, w_{\mathrm{C}}) := \mathrm{Log}(P^{\mathrm{U}}_{\mathrm{C}}(w_{\mathrm{C}}, K_{\mathrm{C}}\, z)) - \mathrm{Log}(w_{\mathrm{C}}) \tag{36}$$

$$q^{\mathrm{L}}_{\mathrm{T}}(z, w_{\mathrm{T}}) := \mathrm{Log}(P^{\mathrm{L}}_{\mathrm{T}}(w_{\mathrm{T}}, K_{\mathrm{T}}\, z)) - \mathrm{Log}(w_{\mathrm{T}}). \tag{37}$$

The description of the EM-type iterative method has been omitted, as its transformation into iterative equations using the notation defined for the experiment is similar to that of the MA-type method.

The parameters were set as follows: the step size h was set to 3 for the MA-type method, 4 for the EM-type, and 1 for the additive-type unless otherwise stated; all penalty coefficients were set to 1; and the parameter α in Equation (28) was set to 0.1. The step size h was varied, depending on the method, to adjust the convergence speed of the iterative process. For example, setting a common value of 1 for all types would still yield qualitatively the same behavior. The initial values for $w_{\mathrm{C}}(0)$ and $w_{\mathrm{T}}(0)$ were chosen as certain values that were either equal to or less than $b^{\mathrm{U}}_{\mathrm{C}}$ and equal to or greater than $b^{\mathrm{L}}_{\mathrm{T}}$, respectively. These initial values were selected as uniform values of 15 for $w_{\mathrm{C}}(0)$ and 52 for $w_{\mathrm{T}}(0)$. We used the variable dose-constraints method to solve the IMRT inverse problems by modifying the open-source treatment planning platform matRad [34]. Each iterative method was executed with the parameter and initial value settings described above, and the sequence of iterates was computed accordingly. The convergence to an acceptable solution was assessed using the collaboration index $\Delta(z(n))$ defined in Equation (23), and the optimization was terminated once this index reached zero. This termination criterion was uniformly applied to all the methods compared. The performance of each method was evaluated based on the evolution of this index and the resulting dose–volume histograms of the final solutions.

4.2. Results and Discussion

First, we present the experimental results of the variable dose-constraints method based on the multiplicative approach. To illustrate the transition of partially acceptable states, Figure 2 plots the volume ratios specified in Equation (6), the acceptability indices, and the collaboration index defined in Equation (23), all as functions of the iteration number n, obtained using the MA-type iterative formula. The upper part of the figure displays $\eta_{\mathrm{C}}^{\mathrm{U}}(z(n))$, $\eta_{\mathrm{T}}^{\mathrm{U}}(z(n))$, $\eta_{\mathrm{T}}^{\mathrm{L}}(z(n))$, and $\eta_{\mathrm{B}}^{\mathrm{U}}(z(n))$, while the lower part shows $\delta_{\mathrm{C}}^{\mathrm{U}}(z(n))$, $\delta_{\mathrm{T}}^{\mathrm{U}}(z(n))$, $\delta_{\mathrm{T}}^{\mathrm{L}}(z(n))$, $\delta_{\mathrm{B}}^{\mathrm{U}}(z(n))$, and $\Delta(z(n))$, arranged from top to bottom. The behavior of collaboration index $\Delta(z(n))$ confirms the transition from multiple partially acceptable states to a fully acceptable state. The iteration count at which $\Delta(z(n))$ reaches zero (denoted as N^*) corresponds to the point of convergence to a fully acceptable solution.

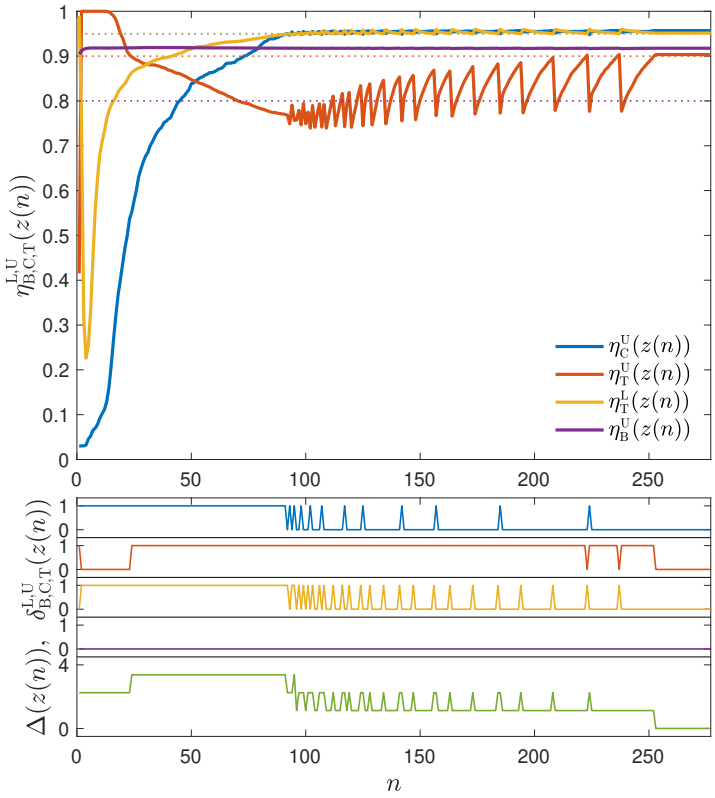


Figure 2. Time evolutions of (upper panel) $\eta_{\mathrm{C}}^{\mathrm{U}}(z(n))$, $\eta_{\mathrm{T}}^{\mathrm{U}}(z(n))$, $\eta_{\mathrm{T}}^{\mathrm{L}}(z(n))$, and $\eta_{\mathrm{B}}^{\mathrm{U}}(z(n))$ and (lower panel) $\delta_{\mathrm{C}}^{\mathrm{U}}(z(n))$, $\delta_{\mathrm{T}}^{\mathrm{U}}(z(n))$, $\delta_{\mathrm{T}}^{\mathrm{L}}(z(n))$, $\delta_{\mathrm{B}}^{\mathrm{U}}(z(n))$, and $\Delta(z(n))$ from top to bottom, obtained using multiplicative MA-type formula.

Additionally, the changes in the acceptability indices $\delta_{\mathrm{C}}^{\mathrm{U}}$ and $\delta_{\mathrm{T}}^{\mathrm{L}}$ affect each other, leading to an oscillatory switching between 0 and 1 during certain iterations. This reflects a cooperative phenomenon between the Core and Target. Not only did $\delta_{\mathrm{B}}^{\mathrm{U}}$ remain at 0 from the beginning, but as a result of this cooperative interaction, both $\delta_{\mathrm{C}}^{\mathrm{U}}$ and $\delta_{\mathrm{T}}^{\mathrm{L}}$ also became 0. Consequently, a dynamical mechanism emerged in which only the upper dose constraint of the Target was partially relaxed, ultimately enabling the entire system to reach an acceptable state.

Figure 3 shows the dose–volume histograms (solid lines) of $K_{\mathrm{C}}\, z(N^*)$ and $K_{\mathrm{T}}\, z(N^*)$ obtained at iteration N^*, where the beam coefficient variable z reached an element of the set $\mathcal{A}$. Additionally, the variable doses $w_{\mathrm{C}}(N^*)$ and $w_{\mathrm{T}}(N^*)$ (dashed lines) are plotted. The fixed dose constraints for the Core and Target were set at an upper limit of 15 Gy and a lower limit of 50 Gy, respectively. Throughout all elements of the dose vector, $w_{\mathrm{C}}(N^*)$ remained lower, while $w_{\mathrm{T}}(N^*)$ remained higher. This behavior indicates that the iterative

system driven by the variable dose-constraints method achieved high-precision IMRT planning by seeking a stricter condition compared with the fixed dose constraints.

The experimental results for the EM-type approach were qualitatively similar to those for when the multiplicative iterative system used the MA-type approach. However, a comparison between Figure 4, which plots the transition of volume ratios and acceptability indices, and Figure 2 reveals a significant difference in how the dynamical system transitioned through partially acceptable states before reaching an acceptable solution. This observation is intriguing as it means that the dose–volume histograms based on the acceptable solutions also differ between the two methods. While both approaches satisfy the prescribed dose–volume constraints, if one aims for stricter conditions within the elements of the acceptable set $\mathcal{A}$, it would be beneficial to try both methods and compare the results.

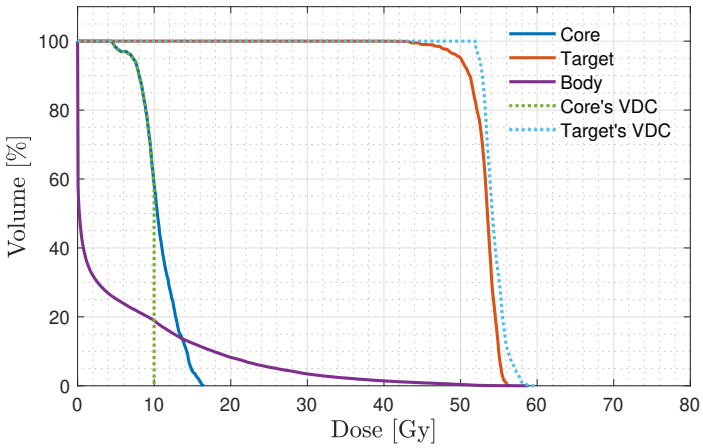


Figure 3. Dose–volume histogram and variable dose constraints (VDCs) obtained using multiplicative MA-type formula.

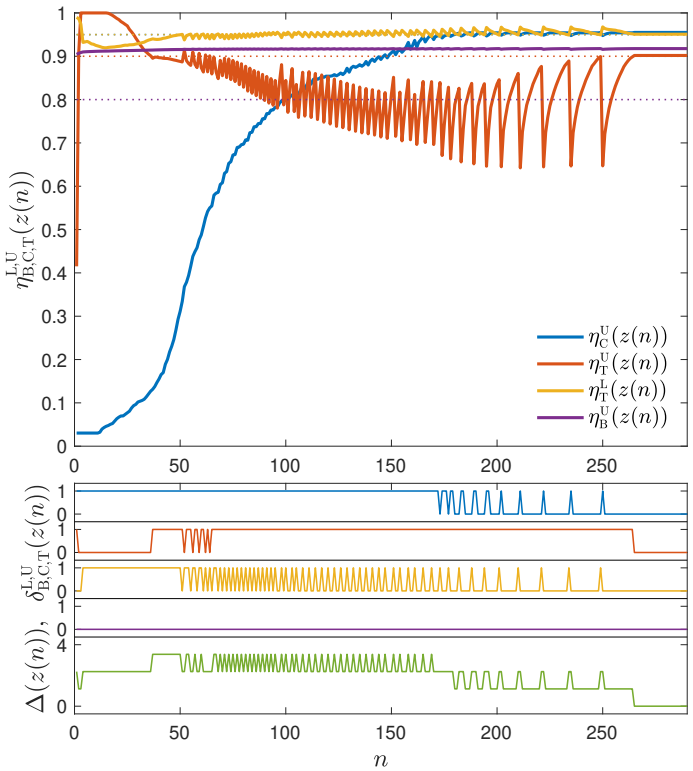


Figure 4. Time evolutions of (upper panel) $\eta^{\mathrm{U}}_{\mathrm{C}}(z(n))$, $\eta^{\mathrm{U}}_{\mathrm{T}}(z(n))$, $\eta^{\mathrm{L}}_{\mathrm{T}}(z(n))$, and $\eta^{\mathrm{U}}_{\mathrm{B}}(z(n))$ and (lower panel) $\delta^{\mathrm{U}}_{\mathrm{C}}(z(n))$, $\delta^{\mathrm{U}}_{\mathrm{T}}(z(n))$, $\delta^{\mathrm{L}}_{\mathrm{T}}(z(n))$, $\delta^{\mathrm{U}}_{\mathrm{B}}(z(n))$, and $\Delta(z(n))$ from top to bottom, obtained using multiplicative EM-type formula.

Next, we considered the differences from the additive approach. Using the same settings as those in the multiplicative approach, we illustrate in Figure 5 the transition process to a feasible solution obtained by the additive iterative scheme given in Reference [24]. In this algorithm, a clipping operation is applied at each iteration to enforce the nonnegativity of the state variables. Although the partially feasible states differ from those of the two types of multiplicative approaches, proper optimization is observed. As information indicating the execution of the clipping operation, Figure 6 presents a bar graph (left axis) showing the number of elements in the state variable $z(n)$ that become zero, along with data series represented by points (right axis) showing the minimum and maximum values of the elements as functions of the iteration number n.

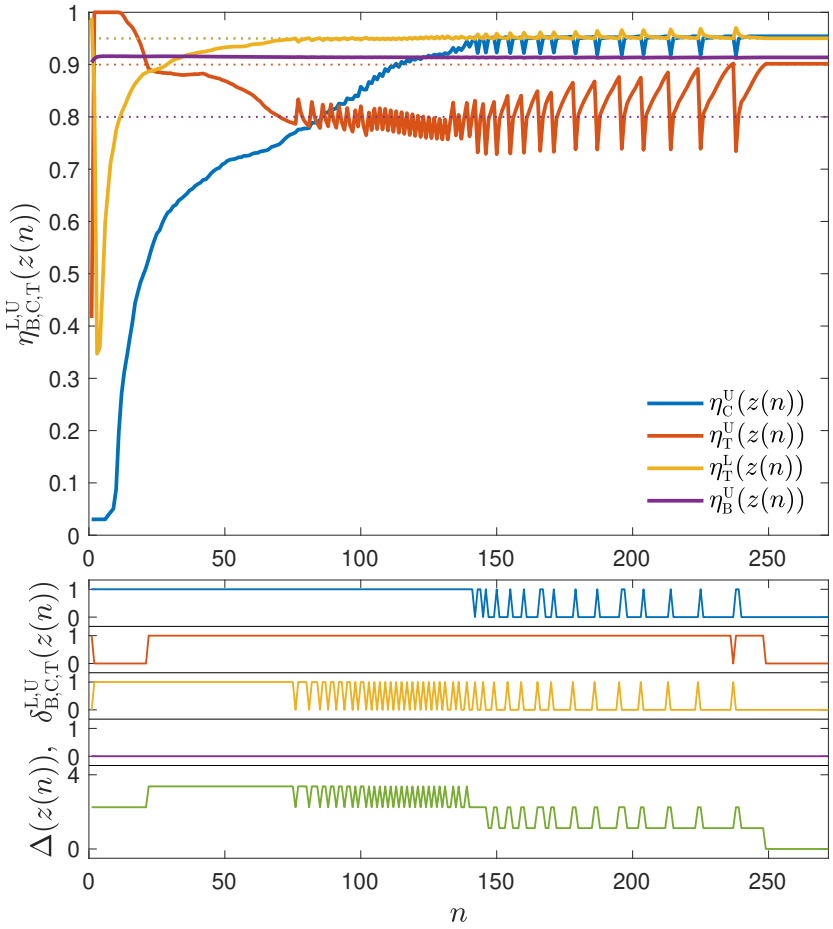


Figure 5. Time evolutions of (upper panel) $\eta^{\mathrm{U}}_{\mathrm{C}}(z(n))$, $\eta^{\mathrm{U}}_{\mathrm{T}}(z(n))$, $\eta^{\mathrm{L}}_{\mathrm{T}}(z(n))$, and $\eta^{\mathrm{U}}_{\mathrm{B}}(z(n))$ and (lower panel) $\delta^{\mathrm{U}}_{\mathrm{C}}(z(n))$, $\delta^{\mathrm{U}}_{\mathrm{T}}(z(n))$, $\delta^{\mathrm{L}}_{\mathrm{T}}(z(n))$, $\delta^{\mathrm{U}}_{\mathrm{B}}(z(n))$, and $\Delta(z(n))$ from top to bottom, obtained using additive formula with clipping procedure.

Our several experiments conducted within the acceptable constraint settings showed no instances in which the clipping operation of the additive iteration system had an inappropriate effect. Therefore, we performed the additive method under more stringent conditions where the entire IMRT system became unacceptable by reducing only the value of the parameter $b^{\mathrm{U}}_{\mathrm{B}}$, which defines the upper dose limit for the Body, as shown in Table 1. To ensure that oscillatory behavior did not arise due to discretization accuracy, the step size h was set to 1 uniformly across all iterative schemes in the experiments. Under these stringent conditions, it was verified that the state variable of the discrete-time dynamical system converged to a stable periodic point. Specifically, the orbit reached a steady state after a sufficiently large number of iterations (2000). For example, when $b^{\mathrm{U}}_{\mathrm{B}}$ took values of 4, 4.34, and 5, periodic points appeared with periods of 2, 7, and 3, respectively. Figure 7

shows the transition of the volume ratio and collaboration index for the case where $b_{\mathrm{B}}^{\mathrm{U}} = 5$. Here, it is evident that the points of the volume ratio change significantly in a periodic manner. Moreover, from the plot in Figure 8, the data series representing the maximum values of the state variable z reflect the points of the state with a period of 3.

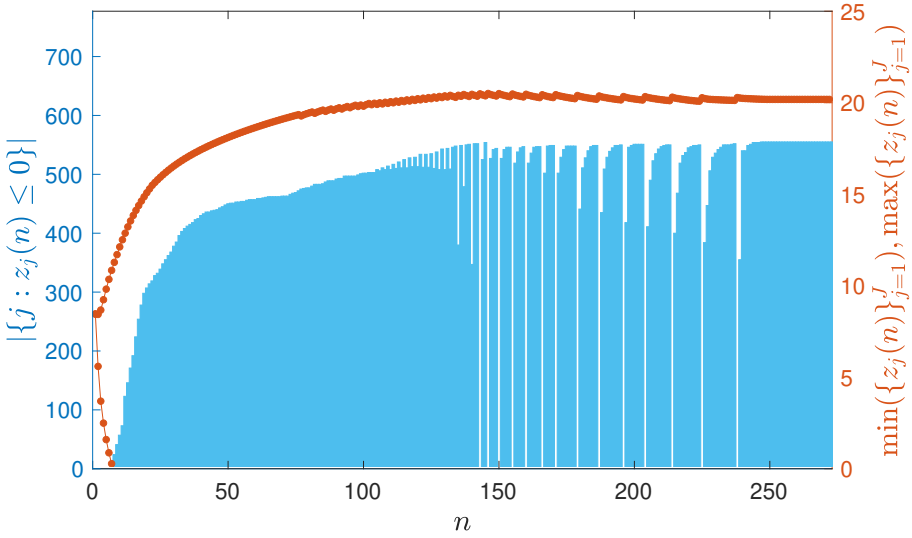


Figure 6. Number of negative elements in $z(n)$ (bars, left axis), along with its minimum and maximum values (markers, right axis), obtained using additive formula.

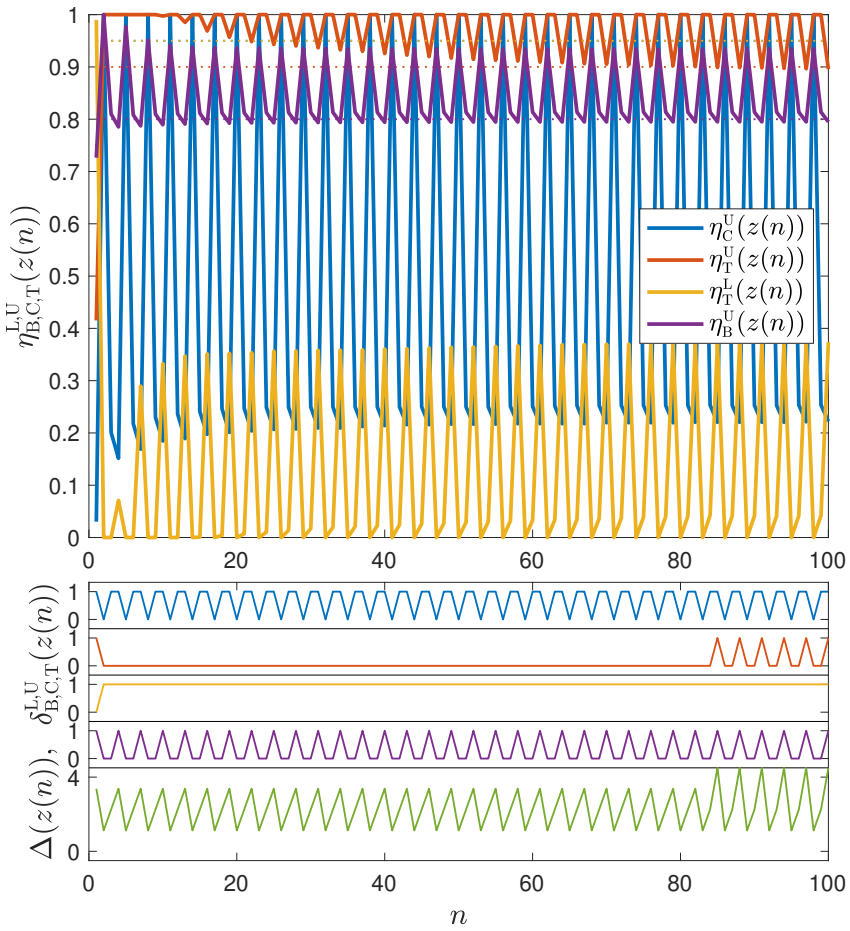


Figure 7. Time evolutions of (upper panel) $\eta_{\mathrm{C}}^{\mathrm{U}}(z(n))$, $\eta_{\mathrm{T}}^{\mathrm{U}}(z(n))$, $\eta_{\mathrm{T}}^{\mathrm{L}}(z(n))$, and $\eta_{\mathrm{B}}^{\mathrm{U}}(z(n))$ and (lower panel) $\delta_{\mathrm{C}}^{\mathrm{U}}(z(n))$, $\delta_{\mathrm{T}}^{\mathrm{U}}(z(n))$, $\delta_{\mathrm{T}}^{\mathrm{L}}(z(n))$, $\delta_{\mathrm{B}}^{\mathrm{U}}(z(n))$, and $\Delta(z(n))$ from top to bottom, obtained using additive formula.

By significantly reducing the value of $b_{\mathrm{B}}^{\mathrm{U}}$ from the acceptable constraint setting, it is considered that the clipping operation affected the solution trajectory. On the other hand, in the multiplicative method, although the volume ratio fluctuated greatly in the early iterations, the state variables asymptotically approached a near-optimal solution, and the steady state did not become periodic. Furthermore, no large fluctuations were observed when an additive iterative algorithm without the clipping operation was tested, supporting that the periodic behavior observed in the clipped case can reasonably be attributed to the presence of the clipping operation, which was the only difference between the two settings.

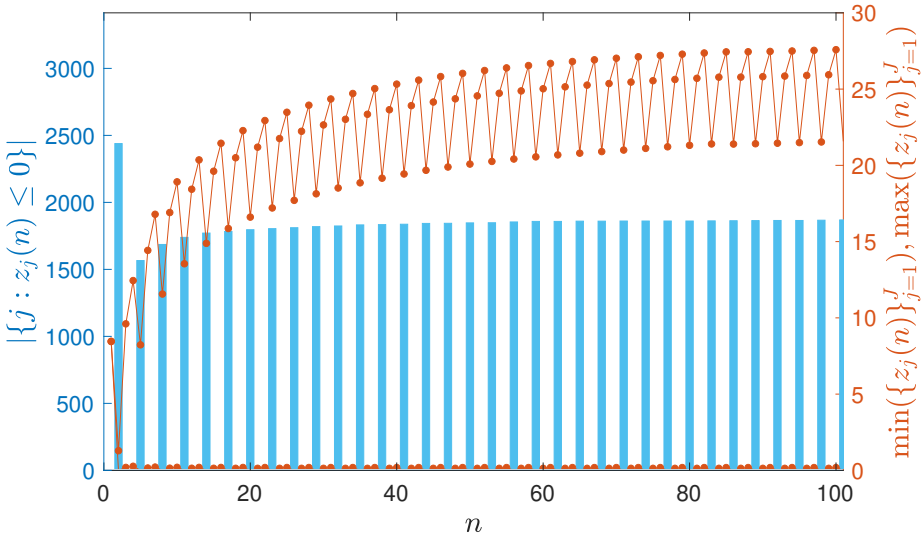


Figure 8. Number of negative elements in $z(n)$ (bars, left axis), along with its minimum and maximum values (markers, right axis), obtained using additive formula.

5. Conclusions

We proposed two types of variable dose-constraints method based on multiplicative iterative schemes for high-precision IMRT planning. Through a theoretical analysis of the differential equation system corresponding to the continuous analog of the iterative scheme, we proved the stability of an equilibrium for consistent IMRT planning by using the Lyapunov theorem. In each multiplicative variable dose-constraints method, the positivity of state variables was confirmed at each iteration. Numerical experiments demonstrated that this method converges to an acceptable solution while maintaining physically meaningful solutions throughout the optimization process. Specifically, under strict dose constraints, whereas the previous additive approach showed undesirable periodic behaviors in the iterative process, the proposed multiplicative method proceeded with the optimization without inducing such fluctuations while preserving nonnegativity. This suggests that it not only ensures constraint satisfaction but also enhances the robustness of the treatment plan. A quantitative characterization of this robustness remains an important direction for future research.

Overall, the proposed method provides a flexible and efficient framework for IMRT planning and offers significant advantages over traditional static approaches based on fixed dose constraints. While detailed performance comparisons between variable and fixed dose-constraints methods have already been presented in our earlier work, the present study addresses specific limitations of previous formulations—namely, the need for lower bound clipping to avoid negative values and the resulting oscillatory behavior. The proposed multiplicative formulation overcomes these issues by ensuring nonnegativity throughout the iterative process and maintaining stable convergence. By promoting both feasibility and

consistency during optimization, the method enhances the reliability of treatment planning and supports broader clinical applicability.

Author Contributions: Conceptualization, T.Y.; Data Curation, T.K., R.N., N.O., K.H. and T.Y.; Formal Analysis, O.M.A.A.-O. and T.Y.; Methodology, O.M.A.A.-O. and T.Y.; Software, T.K. and T.Y.; Supervision, T.Y.; Validation, O.M.A.A.-O., T.K., R.N., N.O., K.H. and T.Y.; Writing—Original Draft, O.M.A.A.-O. and T.Y.; Writing—Review and Editing, O.M.A.A.-O., T.K., R.N., N.O., K.H. and T.Y. All authors have read and agreed to the published version of the manuscript.

Funding: This research was partially supported by JSPS KAKENHI, Grant Number 24K07507.

Data Availability Statement: All data used to support the findings of this study are included within the article.

Conflicts of Interest: The authors declare no conflicts of interest regarding the publication of this paper.

References

1. Palta, J.R.; Mackie, T.R. (Eds.) *Intensity-Modulated Radiation Therapy: The State of the Art*; Medical Physics Publishing: Madison, WI, USA, 2003.
2. Bortfeld, T. IMRT: A review and preview. *Phys. Med. Biol.* **2006**, *51*, R363–R379. [CrossRef] [PubMed]
3. Cho, B. Intensity-modulated radiation therapy: A review with a physics perspective. *Radiat. Oncol. J.* **2018**, *36*, 1. [CrossRef] [PubMed]
4. Mohan, R. Intensity-modulated radiation therapy—You can have your cake and eat it too! *Med. Phys.* **2023**, *50*, 74–79. [CrossRef]
5. Wu, Q.; Mohan, R. Algorithms and functionality of an intensity modulated radiotherapy optimization system. *Med. Phys.* **2000**, *27*, 701–711. [CrossRef] [PubMed]
6. Cotrutz, C.; Lahanas, M.; Kappas, C.; Baltas, D. A multiobjective gradient-based dose optimization algorithm for external beam conformal radiotherapy. *Phys. Med. Biol.* **2001**, *46*, 2161–2175. [CrossRef]
7. Wu, Q.; Mohan, R. Multiple local minima in IMRT optimization based on dose-volume criteria. *Med. Phys.* **2002**, *29*, 1514–1527. [CrossRef] [PubMed]
8. Lahanas, M.; Schreibmann, E.; Baltas, D. Multiobjective inverse planning for intensity modulated radiotherapy with constraint-free gradient-based optimization algorithms. *Phys. Med. Biol.* **2003**, *48*, 2843–2871. [CrossRef]
9. Zhang, X.; Liu, H.; Wang, X.; Dong, L.; Wu, Q.; Mohan, R. Speed and convergence properties of gradient algorithms for optimization of IMRT. *Med. Phys.* **2004**, *31*, 1141–1152. [CrossRef]
10. Censor, Y.; Bortfeld, T.; Martin, B.; Trofimov, A. A unified approach for inversion problems in intensity-modulated radiation therapy. *Phys. Med. Biol.* **2006**, *51*, 2353–2365. [CrossRef]
11. Bortfeld, T.; Kufer, K.H.; Monz, M.; Trofimov, A.; Niemierko, A. Problems with current IMRT prescription practices and planning systems [abstract]. *Med. Phys.* **2004**, *31*, 1761.
12. Bauschke, H.H.; Borwein, J.M. On Projection Algorithms for Solving Convex Feasibility Problems. *SIAM Rev.* **1996**, *38*, 367–426. [CrossRef]
13. Byrne, C. Iterative oblique projection onto convex sets and the split feasibility problem. *Inverse Probl.* **2002**, *18*, 441–453. [CrossRef]
14. Censor, Y.; Chen, W.; Combettes, P.L.; Davidi, R.; Herman, G.T. On the effectiveness of projection methods for convex feasibility problems with linear inequality constraints. *Comput. Optim. Appl.* **2012**, *51*, 1065–1088. [CrossRef]
15. Lougovski, P.; LeNoach, J.; Zhu, L.; Ma, Y.; Censor, Y.; Xing, L. Toward truly optimal IMRT dose distribution: Inverse planning with voxel-specific penalty. *Technol. Cancer Res. Treat.* **2010**, *9*, 629–636. [CrossRef] [PubMed]
16. Fu, A.; Ungun, B.; Xing, L.; Boyd, S. A convex optimization approach to radiation treatment planning with dose constraints. *Optim. Eng.* **2018**, *20*, 277–300. [CrossRef]
17. Mukherjee, S.; Hong, L.; Deasy, J.O.; Zarepisheh, M. Integrating soft and hard dose-volume constraints into hierarchical constrained IMRT optimization. *Med. Phys.* **2019**, *47*, 414–421. [CrossRef]
18. Zhang, T.; Bokrantz, R.; Olsson, J. Direct optimization of dose–volume histogram metrics in radiation therapy treatment planning. *Biomed. Phys. Eng. Express* **2020**, *6*, 065018. [CrossRef]
19. Penfold, S.; Casiraghi, M.; Dou, T.; Schulte, R.W.; Censor, Y. SU-E-T-33: A Feasibility-Seeking Algorithm Applied to Planning of Intensity Modulated Proton Therapy: A Proof of Principle Study. *Med. Phys.* **2015**, *42*, 3338. [CrossRef]
20. Penfold, S.; Zalas, R.; Casiraghi, M.; Brooke, M.; Censor, Y.; Schulte, R. Sparsity constrained split feasibility for dose-volume constraints in inverse planning of intensity-modulated photon or proton therapy. *Phys. Med. Biol.* **2017**, *62*, 3599. [CrossRef]
21. Barkmann, F.; Censor, Y.; Wahl, N. Superiorization of projection algorithms for linearly constrained inverse radiotherapy treatment planning. *Front. Oncol.* **2023**, *13*. [CrossRef]

22. Brooke, M.; Censor, Y.; Gibali, A. Dynamic string-averaging CQ-methods for the split feasibility problem with percentage violation constraints arising in radiation therapy treatment planning. *Int. Trans. Oper. Res.* **2023**, *30*, 181–205. [CrossRef] [PubMed]
23. Aragón-Artacho, F.J.; Censor, Y.; Gibali, A.; Torregrosa-Belén, D. The superiorization method with restarted perturbations for split minimization problems with an application to radiotherapy treatment planning. *Appl. Math. Comput.* **2023**, *440*, 127627. [CrossRef]
24. Obata, N.; Abou Al-Ola, O.M.; Nakada, R.; Kojima, T.; Yoshinaga, T. Variable Dose-Constraints Method for Enhancing Intensity-Modulated Radiation Therapy Treatment Planning. *Mathematics* **2024**, *12*, 3826. [CrossRef]
25. Schropp, J. Using dynamical systems methods to solve minimization problems. *Appl. Numer. Math.* **1995**, *18*, 321–335. [CrossRef]
26. Airapetyan, R.G. Continuous Newton method and its modification. *Appl. Anal.* **1999**, *73*, 463–484. [CrossRef]
27. Ramm, A. Dynamical systems method for solving operator equations. *Commun. Nonlinear Sci. Numer. Simul.* **2004**, *9*, 383–402. [CrossRef]
28. Li, L.; Han, B. A dynamical system method for solving nonlinear ill-posed problems. *Appl. Math. Comput.* **2008**, *197*, 399–406. [CrossRef]
29. Kullback, S.; Leibler, R.A. On Information and Sufficiency. *Ann. Math. Stat.* **1951**, *22*, 79–86. [CrossRef]
30. Gordon, R.; Bender, R.; Herman, G.T. Algebraic reconstruction techniques (ART) for three-dimensional electron microscopy and X-ray photography. *J. Theor. Biol.* **1970**, *29*, 471–481. [CrossRef]
31. Badea, C.; Gordon, R. Experiments with the nonlinear and chaotic behaviour of the multiplicative algebraic reconstruction technique (MART) algorithm for computed tomography. *Phys. Med. Biol.* **2004**, *49*, 1455–1474. [CrossRef]
32. Shepp, L.A.; Vardi, Y. Maximum likelihood reconstruction for emission tomography. *IEEE Trans. Med. Imag.* **1982**, *1*, 113–122. [CrossRef] [PubMed]
33. Vishampayan, S.; Stamos, J.; Mayans, R.; Koral, K.; Clinthorne, N.; Rogers, W.L. Maximum likelihood image reconstruction for SPECT. *J. Nuc. Med. (Abs. Book)* **1985**, *26*, 20.
34. Wieser, H.P.; Cisternas, E.; Wahl, N.; Ulrich, S.; Stadler, A.; Mescher, H.; Muller, L.R.; Klinge, T.; Gabrys, H.; Burigo, L.; et al. Development of the open-source dose calculation and optimization toolkit matRad. *Med. Phys.* **2017**, *44*, 2556–2568. [CrossRef] [PubMed]

Disclaimer/Publisher's Note: The statements, opinions and data contained in all publications are solely those of the individual author(s) and contributor(s) and not of MDPI and/or the editor(s). MDPI and/or the editor(s) disclaim responsibility for any injury to people or property resulting from any ideas, methods, instructions or products referred to in the content.